A model of partially-depleted SOI MOSFETs in the subthreshold range

Daniel Tomaszewski, Lidia Łukasiak, Andrzej Jakubowski, and Krzysztof Domański

Abstract — **A steady-state model of partially-depleted (PD) SOI MOSFETs I-V characteristics in subthreshold range is presented. Phenomena, which must be accounted for in current continuity equation, which is a key equation of the PD SOI MOSFETs model are summarized. A model of diffusion-based conduction in a weakly-inverted channel is described. This model takes into account channel length modulation, drift of carriers in the „pinch-off" region and avalanche multiplication triggered by these carriers. Characteristics of the presented model are shown and briefly discussed.**

Keywords — *SOI MOSFET, subthreshold range, floating body, transconductance.*

1. Introduction

Silicon-on-insulator (SOI) CMOS circuits are predestined for operation at low supply bias and at higher temperatures than their conventional counterparts. These advantages result from the reduced area of p-n junctions, what implies lowered level of junction leakage currents. Therefore these devices exhibit lowered level of power consumption. However, proper operation at low current level is possible only when transistors are carefully designed and manufactured. Thus availability of reliable physical models of PD SOI MOSFETs is important. These models may be used for simulation and characterization purposes.

The aim of this work was to develop a steady-state model of I-V characteristics of the PD SOI MOSFETs. Although several models are already known [1–4], they were derived using assumptions, which are in our opinion, not fully reasonable.

2. DC models of currents in the Si-film

The proposed model is based on the same idea as previously developed DC model of the PD SOI MOSFETs in the strong inversion range [5]. The main equation, which describes its I-V characteristics expresses a total current continuity condition in the device. It is given with formula (1):

$$I_S + I_D = 0 , \qquad (1)$$

where source and drain currents I_S, I_D are given as sums of current components flowing through the electrodes (Eqs. (2), (3))

$$I_S = I_{c,f} + I_{rec,SB} + I_{diff,n,B}(W_{SB}) , \qquad (2)$$

$$I_D = -M_{sat,f} I_{c,f} - M_b \left[I_{gen,DB} + I_{diff,n,B}(L - W_{DB}) \right] . \qquad (3)$$

For the given DC bias point Eq. (1) allows to calculate the floating body-source voltage in the device – a key parameter of the presented model. In the above equations the following components may be mentioned:

$I_{c,f}$ — diffusion current in the weakly inverted channel at the front Si-SiO$_2$ interface; model of this component is described in the next section;

$I_{diff,n,B}$ — diffusion current in the quasi-neutral part of the thin Si-film; this current is accompanied by the recombination of excess minority carriers (electrons) with the excess majority carriers introduced to the Si-film mainly by the avalanche ionization phenomena in the depletion region of surrounding drain area;

$I_{rec,SB}$ — current related to recombination within the space-charge region of the source-body junction;

$I_{gen,DB}$ — current related to generation within the depletion region of the drain-body junction;

$M_{sat,f}$ — coefficient of avalanche multiplication in the „pinch-off" region at the front Si-SiO$_2$ interface;

M_b — coefficient of avalanche multiplication in the depletion region of the drain-body junction.

Body diffusion current $I_{diff,n,B}$ at any coordinate y ($W_{SB} \leq y \leq L - W_{DB}$) is given with the formula (4), where all its parameters have their usual meanings. Factor $W(t_{Si} - W_{GfB} - W_{GbB})$ denotes of course area of diffusion current path. Body diffusion current at the edge of the source-body junction depletion area ($y = W_{SB}$) is contained in the source current. The current at the edge of the drain-body junction depletion area ($y = L - W_{DB}$) is contained in the drain current. Moreover,

$$I_{diff,n,B}(y) = W(t_{Si} - W_{GfB} - W_{GbB}) \, q \frac{D_{n,B}}{L_{n,B}} n_{B,eq} \times$$
$$\times \frac{(e^{V_{BD}/V_{t}-1}) \cosh \frac{y-W_{SB}}{L_{n,B}} - (e^{V_{BS}/V_{t}-1}) \cosh \frac{L-W_{DB}-y}{L_{n,B}}}{\sinh \frac{L-W_{SB}-W_{DB}}{L_{n,B}}} . \qquad (4)$$

Equation (4) is used in models of bipolar transistors to describe transport of minority carriers through base [6]. Moreover, due to the fact, that transistor base is narrow the formula (4) is usually applied in linearized form. However, in case of SOI MOSFETs such approximation cannot be used. The equation (4) was used earlier for the purpose of modelling of PD SOI MOSFETs operation in the strong inversion range [5].

S-B junction recombination and D-B junction generation currents are given with formulae (5) and (6), respectively. They were also used in case of PD SOI MOSFETs in the strong inversion range [5]. They are obtained as solutions of trasport equations in the space-charge areas of the forward or reverse biased p-n junctions, respectively and are based on SRH (Shockley-Read-Hall) model of recombination phenomena. Similarly to the case of diffusion current at the drain generation current is also multiplied by M_b

$$I_{rec,SB} = W\left(t_{Si} - W_{Gf,B} - W_{Gb,B}\right) \frac{kTn_i}{2\tau_J} \sqrt{\frac{\exp\frac{V_{BS}}{V_t} - 1}{V_{bi} - V_{BS}}} \times$$

$$\times\, 2\arctan \frac{\left(\exp\frac{\phi_{F,N}}{V_t} - \exp\frac{V_{BS} - \phi_{F,P}}{V_t}\right) \sqrt{\exp\frac{V_{BS}}{V_t} - 1}}{\exp\frac{V_{BS}}{V_t} - 1 + \left(\exp\frac{\phi_{F,n}}{V_t} + 1\right)\left(\exp\frac{V_{BS} - \phi_{F,P}}{V_t} + 1\right)}, \quad (5)$$

$$I_{gen,DB} = W(t_{Si} - W_{Gf,B} - W_{Gb,B}) \frac{kTn_i}{2\tau_J} \frac{W_{DB}}{2\phi_F - V_{BD}} \sqrt{1 - \exp\frac{V_{BD}}{V_T}} \times$$

$$\times\, \ln\left|\frac{\exp\frac{\phi_F}{V_T} + 1 - \sqrt{1 - \exp\frac{V_{BD}}{V_T}}}{\exp\frac{\phi_F}{V_T} + 1 + \sqrt{1 - \exp\frac{V_{BD}}{V_T}}} \cdot \frac{\exp\frac{V_{BD} - \phi_F}{V_T} + 1 + \sqrt{1 - \exp\frac{V_{BD}}{V_T}}}{\exp\frac{V_{BD} - \phi_F}{V_T} + 1 - \sqrt{1 - \exp\frac{V_{BD}}{V_T}}}\right|. \; (6)$$

3. DC model of current flow at the front interface in the weak inversion range

Well known formula (7) is used in to calculate the current in the weakly inverted channel [7]

$$I_{c,f} = \frac{W}{L_{eff}} \mu_{c,f} V_t \left[Q_{c,f}(L_{eff}) - Q_{c,f}(0)\right]. \quad (7)$$

In the proposed model, however, the channel length modulation is taken into account. This approach is similar to widely used models of MOSFETs operation in saturation range. Intuitively it is obvious, that phenomena in the vicinity of the drain area in subthreshold and saturation ranges should be described in the same way. After all in weak inversion range channel shortening should be even larger than in the saturation range, which is obviously closer to the full strong inversion range. Results of numerical experiments also confirm this thesis [8]. In the presented model three variables: L_{eff}, $Q_{c,f}(0)$, $Q_{c,f}(L_{eff})$ require further evaluation.

Under gradual channel approximation (GCA) conditions $Q_{c,f}(0)$ may be obtained through approximate solution of the 1D Poisson equation, which accounts for minority carriers [7]

$$Q_{cf}(0) \approx$$

$$\approx -\sqrt{2\varepsilon_{Si}qN_B} \frac{\sqrt{V_t}}{2} \exp\left(\frac{-2\phi_F + V_{BS}}{V_t}\right) \frac{\exp\left(\frac{\Psi_{s,f} - \Psi_B}{V_t}\right) - 1}{\sqrt{\frac{\Psi_{s,f} - \Psi_B}{V_t}}}, \quad (8)$$

where surface potential at the front interface $\Psi_{s,f}$ may be obtained using depletion approximation:

$$\Psi_{s,f} - \Psi_B = \frac{\gamma_f^2}{4} \cdot \left[\sqrt{1 + \frac{4}{\gamma_f^2} \cdot (V_{Gf} - V_{FB,f} - \Psi_B)} - 1\right]^2 \quad (9)$$

and Ψ_B denotes potential of the quasi-neutral part of the thin Si-film. Other variables in formulas (8) and (9) have usual meanings.

Similarly to the model of MOSFETs characteristics in the saturation range, at $y = L_{eff}$ GCA conditions remain still valid. Therefore $Q_{c,f}(L_{eff})$ may be obtained using the same method as $Q_{c,f}(0)$. Therefore the following relation may be formulated:

$$Q_{c,f}(L_{eff}) = Q_{c,f}(0) \exp\left(\frac{-V_{c,f}(L_{eff})}{V_t}\right). \quad (10)$$

Here, $V_{c,f}(L_{eff})$ denotes voltage between both ends of the channel. In earlier works [2, 4] minority carriers charge at the drain end of channel was reduced with respect to that at the source according to

$$Q_{c,f}(L) = Q_{c,f}(0) \exp\left(\frac{-V_{DS}}{V_t}\right). \quad (10a)$$

In order to determine mobile carriers charge at the drain end of channel the approach known from the saturation range modelling is used. Similarly to the case of the boundary between strongly inverted channel and „pinch-off" regions the following current continuity condition below threshold at $y = L_{eff}$ may be formulated [7]

$$I_{c,f} = -W\, Q_{c,f}(L_{eff})\, \upsilon_{max}, \quad (11)$$

$$I_{c,f} = \frac{W}{L_{eff}} \mu_{c,f} V_t \left[Q_{c,f}(L_{eff}) - Q_{c,f}(0)\right]. \quad (12)$$

Equation (11) expresses the condition, that in the area between end of channel and drain carriers travel with maximum available velocity υ_{max}. The equations (11) and (12) allow to obtain the following relation between $Q_{c,f}(0)$ and $Q_{c,f}(L_{eff})$ in the subthreshold region:

$$Q_{c,f}(L_{eff}) = \frac{Q_{c,f}(0)}{1 + \frac{\upsilon_{max}L_{eff}}{\mu_{c,f}\, V_t}}. \quad (13)$$

Next, using Eq. (10), $V_{c,f}(L_{eff})$ can be found very easily

$$V_{c,f}(L_{eff}) = V_t \ln\left(1 + \frac{\upsilon_{max}\, L_{eff}}{\mu_{c,f}\, V_t}\right). \quad (14)$$

As expected, in the subthreshold region the voltage drop between the end of the weakly inverted channel and the source (analogous to $V_{DS,sat,f}$ – the saturation voltage at the front Si-SiO$_2$ interface) is low and independent of front gate voltage.

As the last variable necessary for calculation of the subthreshold current according to Eq. (7) effective length L_{eff} of the region where GCA is valid must be determined. It may be calculated approximately using 1D solution of the Poisson equation under full depletion conditions. This is

very similar to the method of estimation of channel length modulation in the saturation range and corresponds to the simplest case of zero electric field at the channel end

$$L_{eff} = L - \sqrt{\frac{2\varepsilon_{Si}}{q N_B} \cdot (V_D - \Psi_{s,f})}. \qquad (15)$$

4. I-V characteristics of the PD SOI MOSFET model in the weak inversion range

I-V characteristics of the PD SOI MOSFET were calculated using the model presented in the previous sections. Parameters of this device are listed in [9, Table 1].

A set of $I(V_{GfS})$ characteristics calculated both for weak and strong inversion and for several values of the drain-source voltage are shown in Fig. 1. These curves illustrate several effects, which are observed both in numerical calculations and in experimental data [2, 3]:

- decrease of the threshold voltage with increasing drain bias,

- increase of the transconductance in the weak inversion range or increasing increase of VDS voltage.
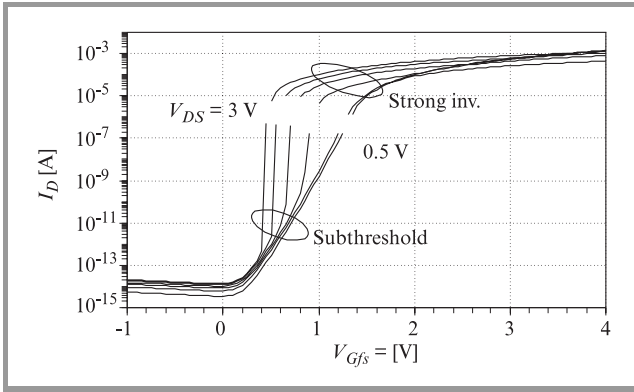

Fig. 1. A family of simulated $I_D(V_{GfS})$ characteristics of the PD SOI MOSFET ($W = 100$ μm, $L = 9.4$ μm, $T_{Oxf} = 32.8$ nm, $T_{Oxb} = 400$ nm, $T_{Si} = 150$ nm, $N_B = 9 \cdot 10^{16}$ cm^{-3}, $V_{GbS} = 0$ V).

Moreover the curves corresponding to the weak and strong inversion ranges, although not connected together, exhibit quite fine transitions between both ranges. This is probably due to the fact, that channel length modulation in the subthreshold range and current conduction close to drain are accounted for in a more proper way. We hope, that the presented approach could help to avoid applying non-physical fitting procedures [4].

Figure 2 shows the behaviour of the thin Si-film potential for varying front gate voltage and for several drain-source voltages. Again variations of threshold voltage is evident and even much more pronounced, than in case of model

with no subthreshold range option. Therefore it may be stated, that even in the weak inversion range, when total current level is low, the floating-body phenomena are also very relevant for the calculation of I-V characteristics of the PD SOI MOSFETs. It results from the fact, that they are still determined by the subtle balance of fluxes of carriers inside the transistor and the channel current in subthreshold range is multiplied by avalanche ionization in the same way as in the strong inversion.
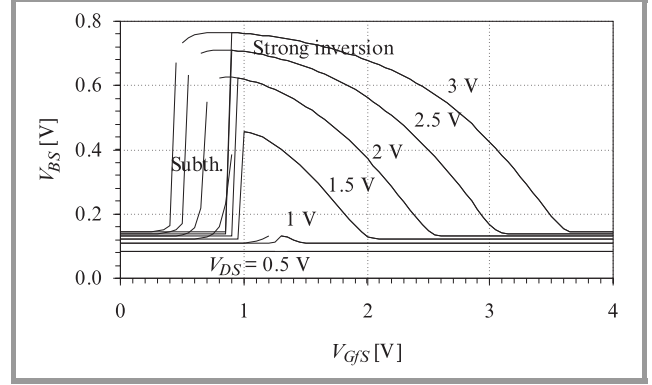

Fig. 2. Comparison of simulated $V_{BS}(V_{GfS})$ characteristics of the PD SOI MOSFET obtained with or without current model in the subthreshold range [5].
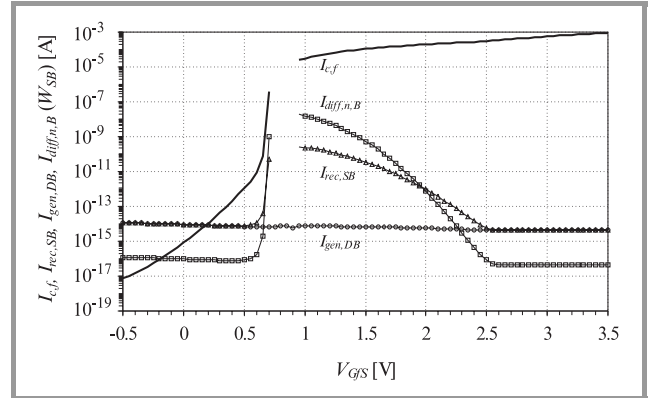

Fig. 3. Comparison of current components in the PD SOI MOSFET (for $V_{DS} = 2$ V): surface diffusion current $I_{c,f}$, bulk diffusion current at the source $I_{diff,n,B}(W_{SB})$, source recombination current $I_{rec,SB}$, and drain generation current $I_{gen,DB}$.

Figure 3 shows comparison of several current components flowing inside the MOSFET in weak and strong inversion ranges: surface diffusion current $I_{c,f}$, bulk diffusion current at the source $I_{diff,n,B}(W_{SB})$, source recombination current $I_{rec,SB}$, and drain generation current $I_{gen,DB}$. The plot shows, that in accumulation range the phenomena in the device are determined entirely by the balance of $I_{diff,n,B}$, $I_{rec,SB}$ and $I_{gen,DB}$ components. The front channel current becomes comparable with them for front gate voltage exceeding 0 V. But it does not reach level, which is sufficient to switch

avalanche-ionization on before V_{GfS} exceeds 0.5 V. Then floating body effects begin to dominate and transistor I-V characteristics exhibit the so-called „kink-effect". In this region a very sharp increase of $I(V_{GfS})$ curve is visible. It is evident that the very high transconductance is strictly correlated with the rapid increase of the body potential, which is in-turn triggered by the avalanche multiplication. Further increase of the front gate voltage results in „smoothing" of the current components variations, because the channel current entirely dominates, so currents balance condition is almost automatically fulfilled. Finally transistors enters the nonsaturation region, when ionization in the „pinch-off" region disappears. Channel current, which dominates is almost proportional to the gate voltage, whereas currents exponentially dependent on body-source voltage decrease by several orders.

5. Conclusions

The paper presents a physical steady-state model of the PD SOI MOSFETs I-V characteristics in the subthreshold range. It accounts for majority of physical effects relevant for proper description of transistors operation. Several model equations were derived on the analogy of saturation range modelling approach. Owing to this, pretty good transition between subthreshold and strong inversion ranges was obtained. Moreover the model exhibits significant decrease of $V_{TH,f}$ for increasing V_{DS} voltage and rapid increase of transconductance for increasing V_{DS} voltage.

Further efforts in this area should be directed towards verification of the model using experimental data and results of numerical calculations using eg. ATLAS/SPISCES simulator. Because PD SOI MOSFETs I-V characteristics may suffer from parasitic edge transistors influence the numerical data may be particularly valuable.

Acknowledgment

References

[1] J.-P. Colinge, *Silicon-on-Insulator Technology: Materials to VLSI*. Kluwer Academic Publishers, 1991.

[2] S. Cristoloveanu and S. S. Li, *Electrical Characterization of Silicon-on-Insulator Materials and Devices*. Kluwer Academic Publishers, 1995.

[3] M. Matloubian, C.-E. D. Chen, B.-Y. Mao, R. Sundaresan, and G. P. Pollack, „Modeling of the subthreshold characteristics of SOI MOSFET's with floating body", *IEEE Trans. Electron Dev.*, vol. 37, no. 9, pp. 1985–1994, 1990.

[4] M. Jurczak, „Modelowanie statycznych charakterystyk prądowo-napięciowych tranzystorów MOS SOI", Ph. D. thesis (in Polish), Warsaw University of Technology, 1997.

[5] D. Tomaszewski, A. Jakubowski, and J. Gibki, „A model of I-V characteristics of partially-depleted SOI MOSFET", *Electron Technol.*, vol. 32, no. 1-2, pp. 96–103, 1999.

[6] S. M. Sze, *Physics of Semiconductor Devices*. 2nd ed. Wiley-Interscience, 1981.

[7] Y. P. Tsividis, *Operation and Modeling of the MOS Transistor*. McGraw-Hill, 1987.

[8] SILVACO, ATLAS User's Manual, Ver. 4.0, June 1995.

[9] D. Tomaszewski, L. Łukasiak, A. Zaręba, A. Jakubowski, „An impact of frequency on capacitances of partially-depleted SOI MOSFETs", *J. Telecommun. Inform. Technol.*, no. 3/4, 2000.

Andrzej Jakubowski – for biography, see this issue, p. 33.

Lidia Łukasiak – for biography, see this issue, p. 34.

Krzysztof Domański, Daniel Tomaszewski – for biography, see this issue, p. 39.